FINITE VOLUME METHOD ANALYSIS OF EROSIVE WEAR IN PEI COMPOSITE

Amit Shrivastava[1], Anshul choudhary [2]

[1] *Mtech Scholer, Mechanical engineering department, SRIT,Jabalpur, Madhyapradesh, India*
[2]*Assistant professor, Mechanical engineering department, SRIT,Jabalpur, Madhyapradesh, India*

ABSTRACT

Tribology especially related with the parameters like friction, wear and lubrication of interacting surfaces that are in relative motion with each other. Wear is damage to solid surface, generally involving progressive loss of material due to relative motion between the surface and a contacting substance or substances. The five main modes of wear are abrasive, adhesive, fretting, erosion and fatigue wear, which are commonly observed in practical situations. The abrasive and erosive wear are most important modes of wear, the wear coefficient (k) in these two modes is at least one to two orders of magnitude greater than the wear coefficients in other wear modes. Also, the abrasive and erosive wears are the most important among all the forms of wear because they contribute almost 74 % of total cost of wear. In present work discrete phase model in CFD has used to predict the erosion rate in PEI composites material. The effect of impact velocity and the impingement angles is studied by comparing the experimented results. The predicted (simulated) and experimentally measured wear profiles are compared. It was observed that in the case of material ULTEM 1000, 2200 and 4000 the impingement angle 90◦ and impact velocity 88m/s, the predicted and experimented profiles were very accurate.

Keywords : Tribology , PEI composites, FEM ,FVM, CFD

1. INTRODUCTION

1.1 Types of wear

1.1.1 Adhesive wear

Adhesive wear is the only universal form of wear; it arises from the fact that, during sliding, regions of adhesive bonding, called junctions, form between the sliding surfaces. If one of these junctions does not break along its original interface, then a chunk from one of the sliding surfaces will have been transferred to the other surface.

1.1.2 Abrasive wear

Abrasive wear is produced by a hard, sharp surface sliding against a softer one and digging out a groove. The abrasive agent may be one of the surfaces or it may be a third component (such as sand particles) Abrasive wear coefficients are large compared to adhesive ones.

1.1.3 Corrosive wear

Corrosive wear arises when a sliding surface is in a corrosive environment, and the sliding action continuously removes the protective corrosion layer, thus exposing fresh surface to further corrosive attack. Corrosive wear occurs as a result of chemical reaction on a wearing surface.

1.1.4 Surface fatigue wear

Surface fatigue wear occurs as result of the formation and growth of cracks. It is the main form of wear of rolling devices such as ball bearings, wheels on rails, and gears.

1.1.5 Erosive wear

Erosive wear is the dominant process and can be defined as the removal of material from a solid surface due to mechanical interaction between the surface and the impinging particles in a liquid stream

1.2 Erosion modes

Two erosion modes are often distinguished in the literature:

A) Brittle erosion
B) Ductile erosion

The erosion modes are depending on the variation in the erosion rate (ER) with impact angle.

If ER goes through a maximum at intermediate impact angles, typically in the range 15◦–30◦, the response of the eroding material is considered ductile.

In contrast, if ER continuously increases with increasing impact angle and attains a maximum at 90◦ (normal impact), the response of the eroding material is brittle .

2. LITERATURE REVIEW

Alfonso Campos-Amezcua & Armando Gallegos-Mun˜oz (2007) [1] used continuous–discrete phase models to predict the erosion rate on surface blades. The effect of vapour mass flow rate, diameter of the particle and solid mass flow rate was studied and the results are by comparing the results obtained by solving CFD problem.
The erosion rate obtained varying diameter of particles shows that the maximum values of erosion rate decrease, while the particles diameter increases.

Liping Dai & Maozheng Yu, Yiping Dai (2007) [2] used the CFD realizable k–ε turbulence model to reduce solid particle erosion in supercritical steam turbine for two nozzle designs with tip end wall contouring and aft-loaded vane profile respectively. The anti-erosion performances of these nozzles were studied and it was concluded that the tip end wall-contouring nozzle meets the demands for both reducing the secondary flow loss and reducing the SPE damage.

A. Gnanavelu & N. Kapur (2009) [3] developed methodology for predicting material wear rates due to slurry erosion. A combination of standard laboratory based experiments (jet impingement test) and Computational Fluid Dynamic (CFD) simulations were used. The predicted and experimentally measured wear profiles were compared. It was observed that in the case of the 90◦ impingement angle and 7.5m/s flow velocity, the predicted and measured profiles were very accurate.

Benedetto Bozzini, Marco E. Ricotti & Claudio Mele (2003) [4] evaluated erosion–corrosion in the bend surface by using multiphase flow model & discrete phase model. Simulation has proposed of erosion–corrosion phenomena in four-phase flows comprising two immiscible liquids, gas and particulate solid. The fluid dynamics of four-phase mixtures has been studied by means of a CFD tool. The FLUENT code has been used in the investigation of solid particle erosion in gas flow.

Yu-Fei Wang & Zhen-Guo Yang (2008) [5] used the Johnson–Holmquist and Johnson–Cook constitutive equation to model the brittle and ductile erosive behaviour. The erosive processes were simulated using explicit dynamic code ANSYS/LS-DYNA and effect of impingement angle, impact velocity and particle penetration on the targets were studied. The erosion rates reveal by this 3-D computational model is found to be consistent with the experimental results.

Yu-Fei Wang & Zhen-Guo Yang (2009) [6] developed an erosion model based on coupling algorithm of SPH and FEM coupled finite element. In this mesh free analysis the impact angle, impact velocity, residual stresses as well as the crater depth and the energy transformation are successfully calculated. In this study, the variation of impact angle and impact velocity in the model was achieved through ANSYS Parametric Design Language (APDL). In this analysis they had found that the maximum erosion rate appeared when the solid particles obliquely impacted the target materials.

K. Shimizu, T. Noguchi & Y. Matsubara (2001)[7] have used Tabor's theory and a general-purpose structural-analysis software (MARC) by a finite element method to analyzed impact angle dependence of plastic deformation on a test piece surface by a single solid particle. Sample materials used were a general structural mild steel of SS400 (henceforth SS400) and ferritic spherical-graphite cast iron (henceforth FDI). They found that maximum wear occurred at 20–30◦ for mild steel, and 60◦ for ductile iron.

Q. Chen & D.Y. Li (2003) [8] used micro-scale dynamic model (MSDM) to simulate solid particle erosion. In this model, the target material and solid particles were discretized and mapped onto a square grid or lattice. Erosion of typical ductile and brittle materials, copper and silicon carbide, were modelled. It was found that the severe lattice distortion and higher damage of both the ductile and brittle materials were existing at impact angles of 30◦ and 90◦ respectively.

M**ariusz Bielawski & Wieslaw Beres (2007) [9]** developed a finite element methodology to investigate tensile stresses in the surface of multilayered coatings under single particle impact. Eight different coating architectures were analyzed to determine reduction in tensile stresses obtained through a combination of layering patterns and material property selections.

I. M. Hutchings (1981)[10] presented a theoretical analysis for the erosion of metals by spheres at normal incidence. This theory explains several features of the erosion of metals by spherical particles at normal impingement, predicts a velocity exponent of 3.0 and incorporates two material strength properties: dynamic hardness and ductility. High values of both are needed for good resistance to erosive wear.

A.P. Harsha & Avinash A. Thakre (2007)[11] investigated the effects of impingement angle and impact velocity on the solid particle erosion behaviour of polyetherimide and its composites. It was found out that the composites were indicating semi ductile erosion behaviour with maximum erosion rate was found in 30-60 impingement angle. The effect of various mechanical properties of the erosion rate of the composite were studied and empirical relations were developed.

3. MODELLING AND ANALYSIS

3.1 INITIAL DESIGN

The modelling of PEI plate has done in GAMBIT modelling software, where all dimensions and conditions have defined.

3.1.1 GEOMETRY GENERATION

- Plate dimension =30x30x3.2 mm
- Nozzle diameter= 4 mm
- Nozzle distance from plate= 10 mm
- Nozzle length= 10mm

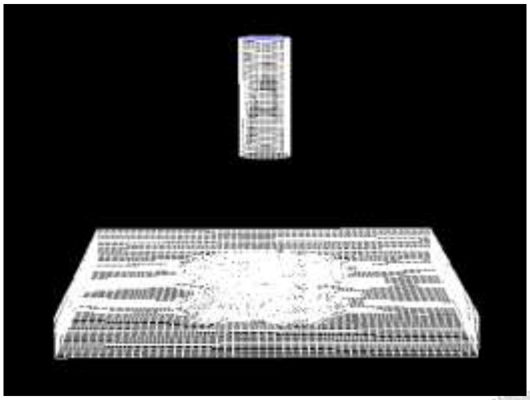

Figure 3.1 Meshed Gambit model

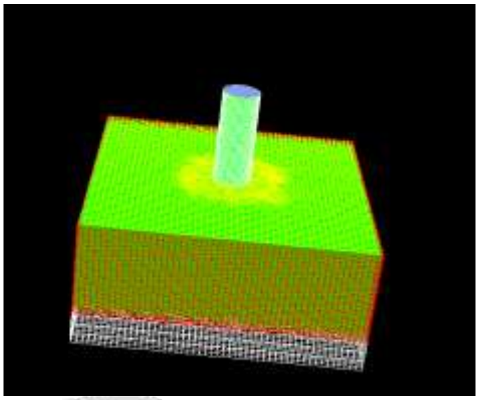

Figure 3.2 Gambit model with boundary conditions

3.1.2 MESH GENERATION

Number of nodes = 348982
Element types = hexahedral brick and quadrilateral

Total no. of element =1344468 (Including inlet, wall, outlet & interior)

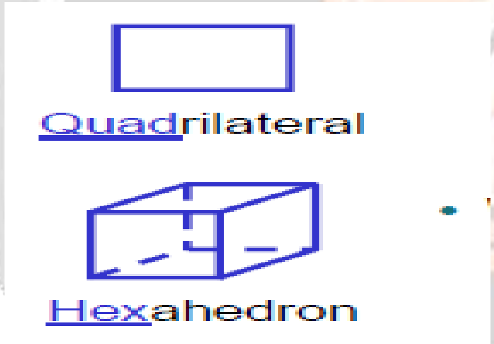

Figure 3.3 Quadrilateral or hexahedral element

3.1.3 Specify Boundary types

Table 3.1 Specification of Boundary Types

Name	Type
inlet	Velocity inlet
Inlet wall	Wall
Side wall	Outflow
Plat, plate wall, lower plate	Wall
Far field	Symmetry

3.2 PREPROCESSING

3.2.1 Simulation Parameters and Boundary Conditions

All parameters have been used for analysis in ANSYS FLUENT.

Table 3.2 Specification of computer model parameters

Parameter	Value or description
Solver type	pressure based/segregated

Air density [kg/m3]	1.225
Air viscosity [kg/ms]	$1.7894*10^{-9}$
Sand density [kg/m3]	2600
Sand diameter [mm]	0.2
Sand particle shape	Spherical
Turbulence model	κ-ε Standard, Standard Wall Function (SWF)
Discrete phase model	Erosion\accretion physical model
Energy equation	switched off
PEI density [kg/m3]	1270, 1420, 1510, 1610, 1370, 1700
Operational pressure [Pa]	101325
Acceleration of gravity [m/s2]	9.81
Inlet type	velocity inlet
Inlet air velocity [m/s]	30, 52, 60, 88
Turbulent intensity (inlet and outlet)	5%
velocity exponent function	2.6
Mass flow rate	4.7 gm/min.= $7.8*10^{-5}$ kg/sec.
Coupled Dispersed Phase	Enabled
Space	3D
Time	Unsteady, 1st-Order Implicit

3.3 SOLVER

There are several methods of discretizing a given differential equation, but finite volume is used in ANSYS-FLUENT. The finite volume method is a numerical method for solving partial differential equations that calculates the values of the conserved variables averaged across the volume. One advantage of the finite volume method over finite difference methods is that it does not require a structured mesh (although a structured mesh can also be used). Furthermore, the finite volume method is preferable to other methods as a result of the fact that boundary conditions. can be applied noninvasively. This is true because the values of the conserved variables are located within the volume element, and not at nodes or surfaces. Finite volume methods are especially powerful on coarse non uniform grids and in calculations where the mesh moves to track interfaces or shocks.

4. RESULTS AND DISCUSSIONS

All geometry parameters are defined in gambit then imported the model in FLUENT software for processing. After defined simulation parameters and boundary conditions for processing, post processor will give the results.

Table 4.1 The caparison between simulated n (velocity exponent) and k(constant) with experimented results

MATERIAL TYPE	IMPINGE-MENT ANGLE (°DEG)	SIMULATED RESULTS			EXPERIMENTED RESULTS		
		k	n	R^2	k	n	R^2
ULTEM 1000	15	5.00E-10	2.6	1	3.00E-08	1.9378	0.9531
	30	2.00E-10	2.8303	0.996	9.00E-09	2.3315	0.862
	60	2.00E-10	2.8872	0.993	9.00E-08	1.7943	0.9532
	90	5.00E-10	2.6028	1	4.00E-09	2.2673	0.9857
ULTEM 2200	15	6.00E-10	2.6031	1	1.00E-08	2.1309	0.9575
	30	3.00E-10	2.7882	0.9973	2.00E-09	2.581	0.9007
	60	9.00E-10	2.6369	0.965	2.00E-07	1.6493	0.8817
	90	6.00E-10	2.603	1	3.00E-09	2.3109	0.9535
ULTEM 2300	15	7.00E-10	2.6013	1	4.00E-09	2.4328	0.9574
	30	7.00E-10	2.602	1	4.00E-09	2.6032	0.924
	60	4.00E-09	2.2682	0.993	6.00E-08	1.9283	0.9633
	90	6.00E-10	2.26046	1	1.00E-07	1.5391	0.8047
ULTEM 2400	15	8.00E-10	2.6011	1	3.00E-08	2.0816	0.9821
	30	9.00E-10	2.6016	1	2.00E-08	2.299	0.8537
	60	4.00E-09	2.2532	0.9887	2.00E-07	1.7233	0.9819
	90	7.00E-10	2.6089	1	1.00E-09	2.7067	0.9888
ULTEM 7801	15	6.00E-10	2.6013	1	7.00E-09	2.3546	0.9591

	30	6.00E-10	2.6017	1	6.00E-09	2.4426	0.953
	60	6.00E-10	3	0.9994	1.00E-07	1.7986	0.9248
	90	5.00E-10	2.6021	1	3.00E-09	2.4625	0.885
ULTEM 4000	15	5.00E-09	2.6009	1	3.00E-07	1.8518	0.9472
	30	5.00E-09	2.601	1	1.00E-07	2.1701	0.91
	60	5.00E-09	2.6443	0.9993	2.00E-07	2.004	0.9686
	90	4.00E-09	3	1	3.00E-06	1.893	0.9959

4.1 CALCULATION OF EROSION RATE

The erosion rate has been calculated as:
Erosion Rate (grams) = DPM Erosion*surface area*1000

Erosion rate (grams) = $kg/m^2 * m^2 * 1000$

$$\text{Erosion rate (g/g)} = \frac{\text{cumulative mass loss of target materials}}{\text{Impact particles weight}}$$

Impact particle weight = testing time ×particle feed rate

Suppose the DPM erosion at impact velocity 30m/s with 15° for material

ULTEM 4000

Erosion rate (grams) = 5.97E-02*πr^2*1000

Erosion rate (g/g) = 3.19E-05

5. CONCLUSIONS

1) The simulated results show that the erosion wear has strong dependence on impact velocity. Increasing the impact velocity the erosion rate increases.

2) The results shows the simulated erosion rate have quit less as compared to experimented results, because of the shape of the sand particles. Spherical shape has been considered for simulation. The shape of particle also plays an important role in erosive wear.

3) The velocity exponent (n) has found 2.5-2.8 in simulated results, which is very much similar to experimented results.

4) The maximum erosion rate found in simulation at impingement angles of 30-60° degree, simulated results shows the semi ductile behavior which is similar to experimental results.

5) Discrete phase model predicted solid particle erosion rate which is very much similar to experimented results. So CFD approach has better to predict erosive wear at any machine components where solid particle or slurry erosion occurred.

REFFERENCES

[1] Alfonso Campos-Amezcua , Armando Gallegos-Mun˜oz , C. Alejandro Romero ,Zdzislaw Mazur-Czerwiec & Rafael Campos-Amezcua Numerical investigation of the solid particle erosion rate in a steam turbine nozzle, Applied Thermal Engineering 27 (2007) 2394–2403.

[2]Liping Dai , Maozheng Yu and Yiping Dai, Nozzle passage aerodynamic design to reduce solid particle erosion of a supercritical steam turbine control stage, Wear 262 (2007) 104–111

[3]A. Gnanavelu, N. Kapur, A. Neville, J.F. Flores, An integrated methodology for predicting material wear rates due to erosion, Wear 267 (2009) 1935–1944

[4]Benedetto Bozzini , Marco E. Ricotti, Marco Boniardi , Claudio Mele, Evaluation of erosion–corrosion in multiphase flow via CFD and experimental Analysis, Wear 255 (2003) 237–245

[5]Yu-Fei Wang, Zhen-Guo Yang, Finite element model of erosive wear on ductile and brittle materials, Wear 265 (2008) 871–878

[6]Yu-Fei Wang, Zhen-Guo Yang, A coupled finite element and meshfree analysis of erosive wear, Tribology International 42 (2009) 373–377

[7]K. Shimizu , T. Noguchi , H. Seitoh , M. Okada, Y. Matsubara, FEM analysis of erosive wear, Wear 250 (2001) 779–784

[8]Q. Chen, D.Y. Li. Computer simulation of solid particle erosion, Wear 254 (2003) 203–210

[9]Mariusz Bielawski , Wieslaw Beres, FE modelling of surface stresses in erosion-resistant coatings under single particle impact, Wear 262 (2007)167–175

[10]I. M. HUTCHINGS**,** A model for the erosion of metals by spherical particles at normal incidence, Wear, 70 (1981) 269 – 281

[11]A.P. Harsha, Avinash A. Thakre, Investigation on solid particle erosion behaviour of polyetherimide and its composites, Wear 262 (2007) 807–818

[12]Tutorial: Using FLUENT's Erosion Model to Investigate Erosion in a 90 degree Elbow Bend.

[13] ANSYS FLUENT 12.0 USER GUIDE, April 2009